

DOI: 10.1002/anie.200502743

Addressing the Metal Centers of  $[2 \times 2]$   $\text{Co}^{\text{II}}_4$  Grid-Type Complexes by STM/STS\*\*Mohammad Sahabul Alam, Stefan Strömsdörfer,  
Viacheslav Dremov, Paul Müller,\* Jens Kortus,  
Mario Ruben,\* and Jean-Marie Lehn\*

The adsorption of functional molecules on solid substrates is increasingly becoming an important aspect of nanoscience and sensing technology. Molecular and supramolecular electronics, understood as the integration of molecular structures to supplement specific functionalities on an integrated circuit chip, is a promising alternative approach for reducing both the feature size and the cost per functional unit. Driven by its characteristic control of the self-assembly process with nanometer accuracy, supramolecular chemistry has a deep impact on the realization of new concepts in molecular electronics. In particular, it plays a leading role in the future development of electronic devices at the solid-state/air interface; the intrinsic physical properties of supramolecular nanostructures can be screened in view of potential applications in nanotechnology.<sup>[1]</sup>

Recent progress in supramolecular coordination chemistry allows access to a broad variety of transition-metal complexes of grid-type architecture comprising two-dimensional arrays of metal ions interconnected by a set of organic

ligands. They appear to be of particular interest as a basis for information storage functions, logic, sensing, and electrical switches.<sup>[2–5]</sup> Complexes of the  $[n \times m]$   $\text{M}^{\text{II}}$  type have been found to exhibit very interesting structural,<sup>[3]</sup> optical,<sup>[4]</sup> magnetic,<sup>[5]</sup> and, in particular the  $[2 \times 2]$   $\text{Co}^{\text{II}}_4$  species, remarkable electronic properties.<sup>[6]</sup>

The synthesis and the structural characteristics of polypyridine-derived, multinuclear metal complexes of the  $[2 \times 2]$   $\text{Co}^{\text{II}}$  grid-type (Figure 1) have been reported earlier.<sup>[7]</sup> The

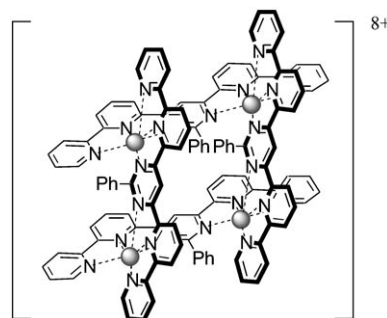


**Figure 1.** Representation of the  $[\text{Co}^{\text{II}}_4\text{L}_4]^{8+}$  complex ( $\text{L} = 4,6\text{-bis}(2,2'\text{-bipyridin-6-yl})\text{-2-phenylpyrimidine}$ ). Each  $\text{Co}^{\text{II}}$  center is coordinated by six N donor atoms (dotted lines).<sup>[6,7]</sup>

central focus of the work presented here is to address two key challenges in the realization of composite solid-state molecule device architectures: the controlled deposition and organization of this class of molecules on solid surfaces and the addressing of individual subunits (here, metal centers) inside the  $[2 \times 2]$   $\text{Co}^{\text{II}}$  grid-type complex.

Experimentally, we applied scanning tunneling microscopy (STM) and scanning tunneling spectroscopy (STS) techniques to free-standing 1D and 2D ensembles as well as to single molecules of the  $[2 \times 2]$   $\text{Co}^{\text{II}}_4$  type deposited onto highly oriented pyrolytic graphite (HOPG). STM studies of densely packed monolayers of  $[\text{Co}^{\text{II}}_4\text{L}_4]^{8+}$  grid complexes on graphite have already been reported.<sup>[8,9]</sup> In order to study the specific features of the electronic properties at the single-molecule level, we concentrated our work on isolated, free-standing molecules. Related work on the investigation of specific functionalities of supramolecular nanostructures on surfaces was reviewed recently.<sup>[10,11]</sup>

Since the structural and electronic informations of STM measurements are strongly entwined,<sup>[12]</sup> the interpretation and analysis of the images of rather complex molecules is not straightforward. In addition, a pure topographical image of the van der Waals surface of  $[2 \times 2]$  grid-like species would not be very useful as it would appear as a more or less featureless “blob” mapping the surface of a pile of more than 200 atoms. However, scanning tunneling spectroscopy (STS) measurements can provide direct information about the molecular energy levels, especially those close to the Fermi level. Functional units of atoms can be distinguished by selective mapping of certain energy regions, provided that their corresponding orbitals are well separated in energy. In general, such STS experiments are carried out under very rigorous conditions (metallic single crystals, ultrahigh-

[\*] MSc M. S. Alam, Dipl.-Phys. S. Strömsdörfer, Dr. V. Dremov, Prof. Dr. P. Müller  
Physikalisches Institut III  
Universität Erlangen-Nürnberg  
Erwin-Rommel-Strasse 1, 91058 Erlangen (Germany)  
Fax: (+49) 9131-15249  
E-mail: phm@physik.uni-erlangen.de

Dr. M. Ruben  
Institut für Nanotechnologie  
Forschungszentrum Karlsruhe GmbH  
76021 Karlsruhe (Germany)  
Fax: (+49) 724-782-6434  
E-mail: mario.ruben@int.fzk.de

Dr. J. Kortus  
Institut de Physique et Chimie des Matériaux de Strasbourg  
23, rue du Loess, BP 43, 67034 Strasbourg (France)  
and  
MPI for Solid-State Research  
Heisenbergstrasse 1, 70569 Stuttgart (Germany)

Prof. Dr. J.-M. Lehn  
ISIS  
Université Louis Pasteur  
8, Allée Gaspard Monge, BP 70028  
67083 Strasbourg cedex (France)  
Fax: (+33) 390-245-140  
E-mail: lehn@isis.u-strasbg.fr

[\*\*] This research was supported by the German Science Foundation through DFG-SFB 583 (P.M.) and the ESF-EUROCORES-SONS project “FunSMARTs” (M.R.). STM: scanning tunneling microscopy, STS: scanning tunneling spectroscopy

vacuum conditions with low temperatures) to minimize the coupling of the system with the environment.<sup>[13]</sup> However, it was also shown that under certain conditions room-temperature STM experiments could detect local changes in the electronic properties of molecules resulting, for example, from intramolecular acceptor–donor,<sup>[14a]</sup> intermolecular  $\pi$ – $\pi$ ,<sup>[14b]</sup> and charge-transfer interactions.<sup>[14c]</sup>

Using a homebuilt STM working under ambient conditions, we succeeded in combining high-resolution topography mapping with simultaneous measurement of current–voltage characteristics (STS) on single molecules deposited on HOPG surfaces. The electrical conductivity of molecules is not only of fundamental interest but is also of considerable significance in device applications.<sup>[15]</sup>

The investigated samples were prepared by depositing a drop of a solution of  $[\text{Co}^{\text{II}}_4\text{L}_4]^{8+}$  molecules in acetonitrile ( $10^{-9}$  M). Different molecular arrangements of Co  $[2 \times 2]$  grid complexes on the HOPG surface could be observed after repeated scanning under relatively mild tunneling conditions (Figure 2). At low coverage the grid complexes get trapped

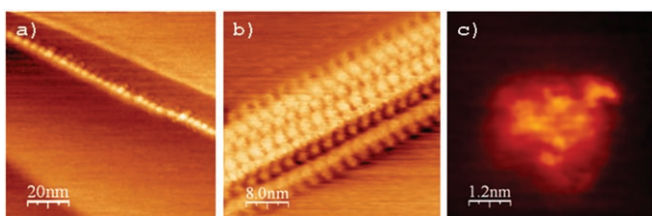


**Figure 2.** STM images of  $[2 \times 2]$   $\text{Co}^{\text{II}}_4$  grid complexes deposited onto a HOPG surface. a) At low concentrations the  $[\text{Co}^{\text{II}}_4\text{L}_4]^{8+}$  complexes are aligned along graphite steps into 1D chains (set point current 5 pA, set point voltage 100 mV). b) 2D crystal formed from  $[\text{Co}^{\text{II}}_4\text{L}_4]^{8+}$  molecules along a graphite step (set point current 200 pA, set point voltage 100 mV). c) An isolated molecule with submolecular resolution (set point current 200 pA, set point voltage 500 mV).

along the step edges of HOPG, and it was possible to obtain continuous 1D chains several hundred nanometers in length (Figure 2a), as well as 2D arrays of densely packed grids (Figure 2b). The ordered 2D structures form spontaneously and start to grow from single nucleation points, which can be considered the 2D equivalent of a crystallization process. At very low coverage, a well-ordered distribution of isolated units is found, even at room temperature where thermal mobility becomes appreciable, which demonstrates the delicate adsorbate–substrate interactions in this system.<sup>[16]</sup>

In Figure 2c, we show a high-resolution STM image of a single  $[2 \times 2]$   $\text{Co}^{\text{II}}_4$  complex. The image appears as a bright uniform spot with a cross-section of about 1.7 nm surrounded by a less defined halo, which can be caused by contributions from the  $\text{BF}_4$  anions and solvent molecules, and corresponds to the molecular size extracted from single-crystal X-ray diffraction studies (1.65 nm).<sup>[7]</sup> Additionally, a quadratic set of slightly brighter spots can be observed on top of the structure anticipating the positions of the cornerstone metal ions. Besides these faint features, as expected, STM topography cannot provide any further information on the intramolecular structure.

In order to investigate the electronic properties of the deposited  $[\text{Co}^{\text{II}}_4\text{L}_4]^{8+}$  molecules, we applied current imaging tunneling spectroscopy (CITS) techniques to the molecule–substrate system. CITS techniques have been developed for scanning tunneling spectroscopy (STS) of a sample surface and consist in the recording of current–voltage ( $I$ – $V$ ) characteristics at every pixel position of the topography map while maintaining a constant tip to surface distance.<sup>[17–19]</sup> The  $I$ – $V$  data set can be sorted such that it provides both a height (topography) map, taken at constant current, and several tens of current (CITS) maps, taken at constant voltage. The current contrast changes significantly when at certain bias voltages new molecular energy levels come into play. Although this technique has been applied successfully to semiconductor materials, its application to organic molecules is rather difficult because of mobility or instability of the molecules, drift, etc.<sup>[20]</sup> Nevertheless, if there would be energy regions where the molecular levels result exclusively from some functional subgroups of atoms, a selective screening of parts of the molecule would be possible.

We successfully applied CITS techniques to the  $[2 \times 2]$   $\text{Co}^{\text{II}}_4$  grid-type complex. We confined our investigations to negative sample-to-tip bias voltages, that is, to the spectroscopy of occupied levels. Figure 3a shows a constant current

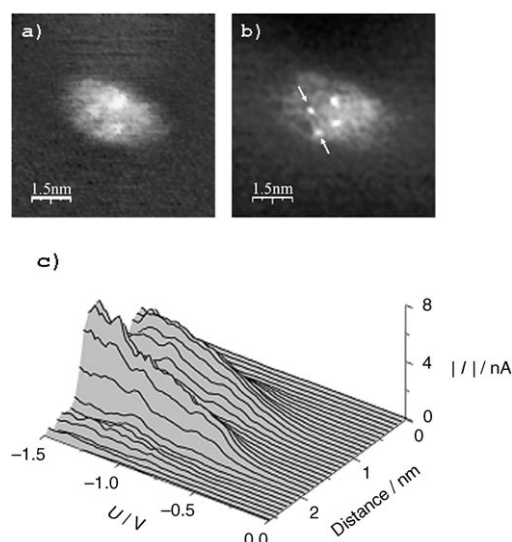


**Figure 3.** a) Topographic map of a  $[2 \times 2]$   $\text{Co}^{\text{II}}_4$  grid. b) Simultaneously recorded current (CITS) image, taken at a voltage of  $-0.942$  V. A quadratic array of bright spots can be detected with a spot-to-spot distance of approximately 0.7 nm. c) Representation of a set of  $I$ – $V$  characteristics measured at positions between the two arrows in Figure 3b.

topography imaging. Figure 3b shows the current map taken at a bias of  $-0.942$  V in the same scan. The tunneling resistance was set to 1 G $\Omega$ . Thereby, the topographic image presents a rather featureless structure with a diameter of approximately 1.7 nm, while the CITS current map reveals a quadratic array of four bright spots representing sharp peaks of the tunneling current. In Figure 3c the set of  $I$ – $V$  characteristics measured at 32 equidistant positions along a

line between the two arrows in Figure 3b is shown. The background current arising from the graphite surface was subtracted. Two ridges are revealed which are approximately 0.7 nm apart. This is in accord to the distance between two neighboring Co ions.<sup>[7]</sup>

Since all distances between the peaks in the CITS pictures correspond to the Co–Co distances in the molecule, we conclude that we have mapped local maxima of the density of states situated at the positions of the Co ions. We note that in spite of the high resolution of the images no features arising from the bis(bipyridyl)pyrimidine ligands were observed. This can be expected because the electronic states of the ligands are located far from the Fermi level  $E_F$ .<sup>[19,21–24]</sup> As a consequence, these states do not play a significant role in the tunneling current at bias voltages down to  $-1.5$  V. This is further confirmed by DFT calculations (vide infra).

Coming back to Figure 3c, we note that below a threshold of approximately  $-0.6$  V the tunneling current at the positions of the bright spots increases drastically. This can be clearly seen in the set of 3D current maps presented in Figure 4.

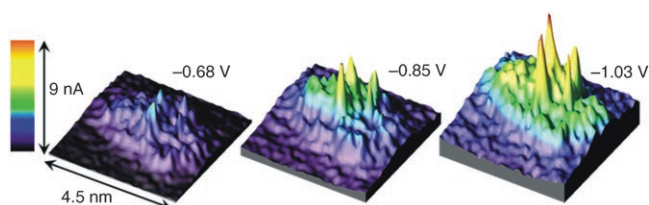


**Figure 4.** Set of 3D current images representing the central part of Figure 3b at different tunnel biases.

The DFT calculations show that the highest occupied molecular orbitals (HOMO) are build from Co d states. The energy gap between the highest occupied and the lowest unoccupied molecular orbital (LUMO) obtained from these calculations is 0.53 eV. The eightfold positively charged grid molecule is highly electronegative. Therefore it seems plausible that the Fermi level will be pinned at the energy position of the LUMO. This would explain the strong increase in tunneling current around  $-0.6$  eV observed experimentally, because tunneling from the HOMO starts at this energy. In the following, all energies are given with respect to the Fermi level. The first three occupied orbitals are quasi degenerate in energy being separated in energy by only a few meV, followed by states at  $-0.55$  and  $-0.60$  eV and sets of states around  $-0.62$  and  $-0.67$  eV. Below  $-0.7$  eV there is an energy gap of about 0.3 eV until the remaining states which exhibit d character are found around  $-1$  eV. As evidenced by Figure 5a, all these states are localized near the position of the Co atoms. Figure 5a shows a superposition of the crystal structure, the above-mentioned orbitals in an energy window between the Fermi level and  $-0.7$  eV (in red), and a color-coded contour plot of the electron density corresponding to these orbitals at a plane parallel to the Co atoms at a distance of 7 Å (white halo around the orbitals). A 3D representation of the electron density maps is repeated in Figure 5b, upper row, using the same coloring scheme as the experimental data.

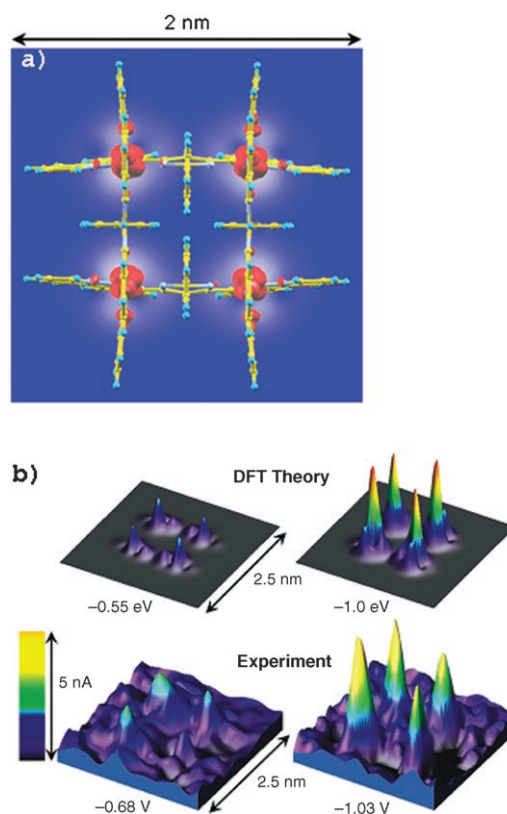


**Figure 5.** a) DFT calculation of occupied orbitals within an energy window between  $E_F$  and  $-0.7$  eV and the electron density map in superposition with the crystal structure data. b) 3D representation of DFT-calculated electron density maps within an energy window between  $E_F$  and  $-0.55$  eV and between  $E_F$  and  $-1$  eV (upper row). Lower row: Central section of the measured CITS maps of Figure 4.

Two energy windows are shown: The first one covers the range between  $E_F$  and the HOMO ( $-0.55$  eV), while the second one covers the full range between  $E_F$  and all states exhibiting 3d character ( $-1$  eV). Considering that DFT usually underestimates band gaps, the HOMO–LUMO gap seems to be underestimated by 150 meV compared to experiment. If one assumes the validity of the Tersoff–Hamann approximation, the theoretical distribution at  $-0.55$  eV should then conform to the map of tunneling currents at a bias of  $-0.7$  eV, etc. The lower row of Figure 5b shows the central part of the CITS current maps of Figure 4 with subtracted background. The accordance with the electron density maps from the DFT calculation is striking. Of course, the DFT calculations do not include possible interactions between molecule and substrate. This might account for some of the discrepancies between theory and measurements.

Intuitively, one would assume that the weakest bonds, in other words, the supramolecular coordination interactions, should dominate the molecular orbitals near the Fermi level of the molecule. A comparison of our measurements with the DFT calculations confirms clearly this assumption. Thus, STS spectroscopy directly addresses the metal centers in a rather complex (supra)molecular entity. If this explanation can be applied also to other supramolecular species with metal centers, our method would allow a selective mapping of the

functional units within the supramolecular architecture, even if these units are embedded into a complex set of organic ligands.

In conclusion,  $[2 \times 2]$   $\text{Co}^{\text{II}}_4$  grid-type complexes on HOPG substrates were imaged using STM with submolecular resolution. At very low coverage, the molecules were shown to align preferably with the step edges of the HOPG surface. The size of the molecules observed is in agreement with the data determined by X-ray crystallography. STS measurements at room temperature allowed us to address directly the metal centers of the supramolecular architectures at the expected locations and in agreement with DFT calculations. It is to be expected that single-molecule spectroscopic techniques such as CITS, together with break junction techniques<sup>[25]</sup> or spin-polarized STM,<sup>[26]</sup> might constitute a significant part of the future tool kit needed for achieving the directed construction and controlled manipulation of fully electronically functional molecular designs.

## Experimental Section

**STM measurements:** All measurements were carried out with a homebuilt low-drift STM head equipped with commercially available low-current-control electronics (RHK technology) under ambient conditions. For high-resolution STM studies a HOPG substrate was freshly cleaved. Afterwards, the substrate was imaged by STM to characterize the tip resolution. We calibrated distances in the STM images by observing atomic spacing on highly oriented pyrolytic graphite (HOPG). After imaging the graphite surface successfully, we deposited a droplet of a solution of the molecule under study and let the droplet run down the graphite surface. Concentrations were around  $10^{-9}$  M. Typically for the STM measurements, tunneling currents between 5 and 200 pA were employed. The bias voltage was between  $\pm 50$  and  $\pm 500$  mV. The scan frequency was varied between 2 and 5 Hz. Resolution was  $256 \times 256$  points for topography, and  $128 \times 128$  in the STS measurements. In STS mode, current-voltage ( $I$ - $V$ ) curves were recorded simultaneously with a constant-current STM image with the interrupted-feedback loop technique. The scan range of voltages was typically from  $-1.5$  to  $0.1$  V relative to the tip potential. Typically, tunneling resistances of the order of  $1 \text{ G}\Omega$  were set. We used mechanically cut Pt-Ir (90:10) tips from wires with a diameter of 0.25 mm. Figures 2, 3a, b, 4, and 5 were produced using the program WSxM (Nanotec Electrónica, Madrid). The molecule  $[\text{Co}^{\text{II}}_4\text{L}_4](\text{BF}_4)_8$  was synthesized as described previously.<sup>[7]</sup>

**DFT calculations:** The first-principles density functional theory (DFT) calculations have been carried out using the Naval Research Laboratory Molecular Orbital Library (NRLMOL) program package, which is an all-electron implementation of DFT. NRLMOL combines large Gaussian orbital basis sets, numerically precise variational integration, and an analytic solution of Poisson's equation in order to accurately determine the self-consistent potentials, secular matrix, total energies, and Hellmann-Feynman-Pulay forces.<sup>[27]</sup> Starting from the X-ray structure, we generated an isolated single Co  $[2 \times 2]$  grid molecule without counterions for the calculation. This resulted in a cluster of 228 atoms used for the DFT calculation. To reduce the numerical cost we used a  $D_2$  symmetry found in the isolated cluster. The basis set for each Co contained 11 s-like, 5 p-like, and 4 d-like contracted Gaussian orbitals with 20 exponents ranging from 0.048 to  $4.2 \times 10^6$ . Nitrogen and carbon had the same number of contracted orbitals (8 s, 4 p, and 3 d), with 13 bare Gaussians between  $0.094$  and  $5.17 \times 10^4$  for N and 12 bare Gaussians between  $0.077$  and  $2.22 \times 10^4$  for C. Finally, hydrogen had 6 s-like, 3 p-like, and 1 d-like orbital with six exponents between  $0.074$  and  $77.84$ . For all orbitals not corresponding to an atomic orbital we used the longest ranged single

Gaussians. This basis set resulted in a total number of 3372 orbitals for each symmetry representation of the complete cluster. The calculations have been carried out for the charged  $8+$  state using the generalized gradient approximation of Perdew, Burke, and Ernzerhof<sup>[28]</sup> to the exchange and correlation functional. The self-consistent charge density was obtained from a spin-polarized calculation with antiferromagnetic order of the Co ions on a dense real-space grid. The figure corresponds to a cut plane parallel to the Co atoms at a distance of  $7 \text{ \AA}$ .

Received: August 4, 2005

Published online: ■ ■ ■ ■ ■, ■ ■ ■ ■ ■

**Keywords:** density functional calculations · scanning probe techniques · self-assembly · supramolecular chemistry · surface chemistry

- [1] a) J.-M. Lehn, *Supramolecular Chemistry. Concepts and Perspectives*, VHC, Weinheim, **1995**, chap. 9 and p. 200; b) J.-M. Lehn, *Science* **2002**, 295, 2400; J.-M. Lehn, *Proc. Natl. Acad. Sci. USA* **2002**, 99, 4763.
- [2] M. Ruben, J. Rojo, F. J. Romero-Salguero, L. H. Uppadine, J.-M. Lehn, *Angew. Chem.* **2004**, 116, 3728; *Angew. Chem. Int. Ed.* **2004**, 43, 3644; M. Ruben, *Angew. Chem.* **2005**, 117, 1620; *Angew. Chem. Int. Ed.* **2005**, 44, 1594.
- [3] Structural properties: P. N. W. Baxter, J.-M. Lehn, J. Fischer, M.-T. Youinou, *Angew. Chem.* **1994**, 106, 2432; *Angew. Chem. Int. Ed. Engl.* **1994**, 33, 2284; P. N. W. Baxter, J.-M. Lehn, G. Baum, D. Fenske, *Angew. Chem.* **1997**, 109, 2067; *Angew. Chem. Int. Ed. Engl.* **1997**, 36, 1978; M. Barbiou, J.-M. Lehn, *J. Am. Chem. Soc.* **2003**, 125, 10257.
- [4] Optical properties: M. Ruben, J.-M. Lehn, G. Vaughan, *Chem. Commun.* **2003**, 1338.
- [5] Magnetic properties: O. Waldmann, J. Hassmann, P. Müller, G. S. Hanan, D. Volkmer, U. S. Schubert, J.-M. Lehn, *Phys. Rev. Lett.* **1997**, 78, 3390; E. Breuning, M. Ruben, J.-M. Lehn, F. Renz, Y. Garcia, V. Ksenofontov, P. Gütllich, E. Wegelius, K. Rissanen, *Angew. Chem.* **2000**, 112, 2563; *Angew. Chem. Int. Ed.* **2000**, 39, 2504; M. Ruben, E. Breuning, J.-M. Lehn, V. Ksenofontov, F. Renz, P. Gütllich, G. Vaughan, *Chem. Eur. J.* **2003**, 9, 4422; M. Ruben, U. Ziener, J.-M. Lehn, V. Ksenofontov, P. Gütllich, G. B. M. Vaughan, *Chem. Eur. J.* **2005**, 11, 94.
- [6] Electronic properties: a) M. Ruben, E. Breuning, J.-P. Gisselbrecht, J.-M. Lehn, *Angew. Chem.* **2000**, 112, 4312; *Angew. Chem. Int. Ed.* **2000**, 39, 4139; b) M. Ruben, E. Breuning, M. Barboiu, J.-P. Gisselbrecht, J.-M. Lehn, *Chem. Eur. J.* **2003**, 9, 291; D. M. Bassani, J.-M. Lehn, S. Serroni, F. Puntoriero, S. Campagna, *Chem. Eur. J.* **2003**, 9, 5936.
- [7] J. Rojo, F. J. Romero-Salguero, J.-M. Lehn, G. Baum, D. Fenske, *Eur. J. Inorg. Chem.* **1999**, 1421.
- [8] A. Semenov, J. P. Spatz, J.-M. Lehn, C. H. Weidl, U. S. Schubert, M. Möller, *Appl. Surf. Sci.* **1999**, 144-145, 456; A. Semenov, J. P. Spatz, M. Möller, J.-M. Lehn, B. Sell, D. Schubert, C. H. Weidl, U. S. Schubert, *Angew. Chem.* **1999**, 111, 2701; *Angew. Chem. Int. Ed.* **1999**, 38, 2547.
- [9] U. Ziener, J.-M. Lehn, A. Mourran, M. Möller, *Chem. Eur. J.* **2002**, 8, 951.
- [10] S. De Feyter, F. C. De Schryver, *Chem. Soc. Rev.* **2003**, 32, 139.
- [11] P. Samorí, *Chem. Soc. Rev.* **2005**, 34, 551.
- [12] Ó. Paz, I. Brihuega, J. M. Gómez-Rodríguez, J. M. Soler, *Phys. Rev. Lett.* **2005**, 94, 056103.
- [13] a) W. Ho, *J. Chem. Phys.* **2002**, 117, 11033; b) P. Wahl, L. Diekhöner, M. A. Schneider, L. Vitali, G. Wittich, K. Kern, *Phys. Rev. Lett.* **2004**, 93, 176603.

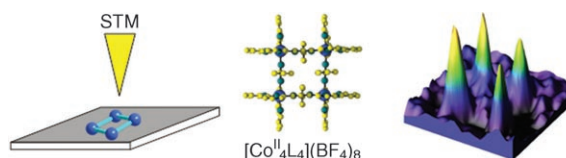
- [14] a) A. Miura, Z. Chen, H. Uji-i, S. De Feyter, M. Sdanowska, P. Jonkhejm, A. P. H. J. Schenning, B. Mejer, F. Würthner, F. C. De Schryver, *J. Am. Chem. Soc.* **2003**, *125*, 14968; b) A. Gesquiere, S. De Feyter, F. C. De Schryver, *Nano Lett.* **2001**, *1*, 201; c) F. Jäckel, M. D. Watson, K. Müllen, J. P. Rabe, *Phys. Rev. Lett.* **2004**, *92*, 188303.
- [15] S. Datta, W. Tian, S. Hong, R. Reifengerger, J. I. Henderson, C. P. Kubiak, *Phys. Rev. Lett.* **1997**, *79*, 2530; R. E. Palmer, Q. Guo, *Phys. Chem. Chem. Phys.* **2002**, *4*, 4275.
- [16] J. V. Barth, J. Weckesser, C. Cai, P. Günter, L. Bürgi, O. Jeandupeux, K. Kern, *Angew. Chem.* **2000**, *112*, 1285; *Angew. Chem. Int. Ed.* **2000**, *39*, 1230.
- [17] R. J. Hamers, R. M. Tromp, J. E. Demuth, *Phys. Rev. Lett.* **1986**, *56*, 1974.
- [18] S. Novokmet, M. S. Alam, V. Dremov, F. W. Heinemann, P. Müller, R. Alsfasser, *Angew. Chem.* **2005**, *117*, 813; *Angew. Chem. Int. Ed.* **2005**, *44*, 803.
- [19] A. M. Ako, H. Maid, S. Sperner, S. H. H. Zaidi R. W. Saalfrank, M. S. Alam, P. Müller, F. W. Heinemann, *Supramol. Chem.* **2005**, *17*, 315.
- [20] M. Rivera, R. L. Williamson, M. J. Miles, *J. Vac. Sci. Technol. B* **1996**, *14*, 1472.
- [21] Z. Klusek, W. Kozłowski, *J. Electr. Spect. Relat. Phenom.* **2000**, *107*, 63.
- [22] D. P. E. Smith, *J. Vac. Sci. Technol. B* **1991**, *9*, 1119.
- [23] H. Nejoh, *Appl. Phys. Lett.* **1990**, *57*, 2907.
- [24] M. Shigeno, M. Ohmi, M. Suginoya, W. Mizutani, *Mol. Cryst. Liq. Cryst.* **1991**, *199*, 141.
- [25] M. A. Reed, C. Zhou, C. J. Muller, T. P. Burgin, J. M. Tour, *Science* **1997**, *278*, 252.
- [26] M. Bode, *Rep. Prog. Phys.* **2003**, *66*, 523; A. R. Smith, R. Yang, W. R. L. Lambrecht, A. Dick, J. Neugebauer, *Surf. Sci.* **2004**, *561*, 154.
- [27] M. R. Pederson, K. A. Jackson, *Phys. Rev. B* **1990**, *41*, 7453; K. A. Jackson, M. R. Pederson, *Phys. Rev. B* **1990**, *42*, 3276; D. V. Porezag, M. R. Pederson, *Phys. Rev. A* **1999**, *60*, 2840; M. R. Pederson, D. V. Porezag, J. Kortus, D. C. Patton, *Phys. Status Solidi B* **2000**, *217*, 197.
- [28] J. P. Perdew, K. Burke, M. Ernzerhof, *Phys. Rev. Lett.* **1996**, *77*, 3865.

## Communications

### Surface Chemistry

M. S. Alam, S. Strömsdörfer, V. Dremov,  
 P. Müller,\* J. Kortus, M. Ruben,\*  
 J.-M. Lehn\* ————— ■■■■-■■■■

Addressing the Metal Centers of  $[2 \times 2]$   
 $\text{Co}^{\text{II}}_4$  Grid-Type Complexes by STM/STS



**The controlled deposition** of grid-type  $[2 \times 2]$   $\text{Co}^{\text{II}}_4$  complexes onto graphite rendered free-standing 0D, 1D, and 2D molecular arrangements, which were examined by STM techniques. STS investigations enabled the direct

addressing of the metal centers at the single-molecule level (see image). The experimentally determined intramolecular positions of the  $\text{Co}^{\text{II}}$  centers are in agreement with DFT calculations of the molecule.